www.
geojournals.cn/georev

墨西哥北部拉拉米期斑岩型铜矿床时空分布及典型矿床特征

姚春彦[1)],郭维民[1)],丁海峰[2,3)],刘君安[1)],王天刚[1)]

1)中国地质调查局南京地质调查中心,南京,210016;2)可持续发展大数据国际研究中心,北京,100094;
3)中国科学院空天信息创新研究院数字地球重点实验室,北京,100094

内容提要:北美斑岩型铜矿集区“大集群”是世界重要铜成矿省之一;墨西哥北部索诺拉州斑岩型铜矿带,是其在墨西哥的延伸。斑岩型铜矿床主要沿着拉拉米岩浆弧展布。拉拉米造山作用期间(80~40 Ma),由于法拉隆板块向北美板块俯冲角度的减小,岩浆活动中心逐步向东移动,形成76~70 Ma, 63~57 Ma和46~40 Ma三期岩浆活动高峰期,其中63~57 Ma岩浆活动规模最大。通过对区内已有矿床的成矿时代与岩浆活动时限及矿床分布集中程度的对比研究发现,斑岩型铜成矿高峰期主要集中在63~56 Ma期间。通过典型矿床的成矿特征梳理及区域岩浆作用综合分析,笔者等认为拉拉米造山作用是区内形成巨量铜钼富集的主要地质作用。

关键词:拉拉米造山运动;斑岩铜矿床;时空分布;墨西哥北部

斑岩型铜矿是世界上最重要的一种矿床类型,以其规模巨大、埋藏浅、矿石成分简单、易开采等特点长期以来是世界铜的主要来源(Cooke et al., 2005; 杨超等, 2020)。世界上大多数斑岩型铜矿床分布于岩浆弧环境,其形成与俯冲作用有关的岩浆活动有关(Hou Zengqian et al., 2003; Richards, 2009;杨志明等,2020)。从全球分布来看,斑岩型铜矿除分布在特提斯—喜马拉雅和古亚州成矿域之外,主要分布在环太平洋中—新生代成矿域(Mutschler et al., 2000; 杨超等, 2020)。北美及南美西科迪勒拉山脉沿线广泛分布着该类型矿床。在北美洲,美国西南部的亚利桑那州和新墨西哥州以及墨西哥西北部的索诺拉州是铜资源最丰富的地区(Titley, 1995),三个地区也被称为北美斑岩型铜矿集区“大集群”(Keith and Swan, 1995),是世界重要的铜产区之一。大型铜矿集群与影响北美西部大部分地区,形成加拿大落基山(Rocky Mountain)褶皱冲断带、美国拉拉米隆起和墨西哥东马德雷褶皱逆冲带的拉拉米(Laramide)造山运动(80~40 Ma)有关,成矿时代多形成于晚白垩世—始新世(Coney and Reyonlds, 1977)。

墨西哥地处北美洲北科迪勒拉南段,北部地区属于北美斑岩型铜矿集区“大集群”,虽然斑岩型铜矿集区“大集群”的概念早就被业界认可并用于矿产勘查中,但是关于铜矿集群的时空分布与岩浆的关系以及单个矿床的对比研究较少。笔者等在综合梳理墨西哥北部拉拉米期岩浆演化特征及斑岩型铜矿分布特征的基础上,结合区内典型铜矿床成矿特征,分析墨西哥北部斑岩型铜矿床时空分布与拉拉米岩浆活动的耦合关系,为墨西哥区域成矿对比研究及矿产勘查提供基础信息。

1 墨西哥大地构造格架

从全球构造演化背景上来看墨西哥地处太平洋的科卡板块与大西洋的加勒比板块之间,属双向俯冲带之间的隆起地块,形成南科迪勒拉褶皱带和墨西哥湾沿岸向斜两大构造单元。墨西哥大地构造演化主要受两个构造作用控制:① 裂谷作用形成的走滑断裂,地壳减薄形成墨西哥湾,并触发了初始的酸性及基性火山活动。② 中生代以来太平洋边缘几乎一直经历俯冲作用,并且不停的发生变化,引起了火山弧的迁移。汇聚边缘板块超俯冲裂谷及收缩作

注:本文为科技部“环太平洋和非洲成矿域战略性矿产信息及成矿规律”项目(编号:2021YFC2901804)和地质调查“美洲大洋洲国际合作地质调查”项目(编号:中地调审[2022]0135)的成果。

收稿日期:2022-07-01;改回日期:2022-08-11;网络首发:2022-09-20;责任编辑:刘志强。Doi: 10.16509/j.georeview.2022.09.061

作者简介:姚春彦,女,1980年生,博士,高级工程师,主要从事地球化学研究;Email: ycyan@126.com。通讯作者:王天刚,男,1983年生,博士,高级工程师,主要从事矿床地质研究;Email: wangtg1897@163.com。

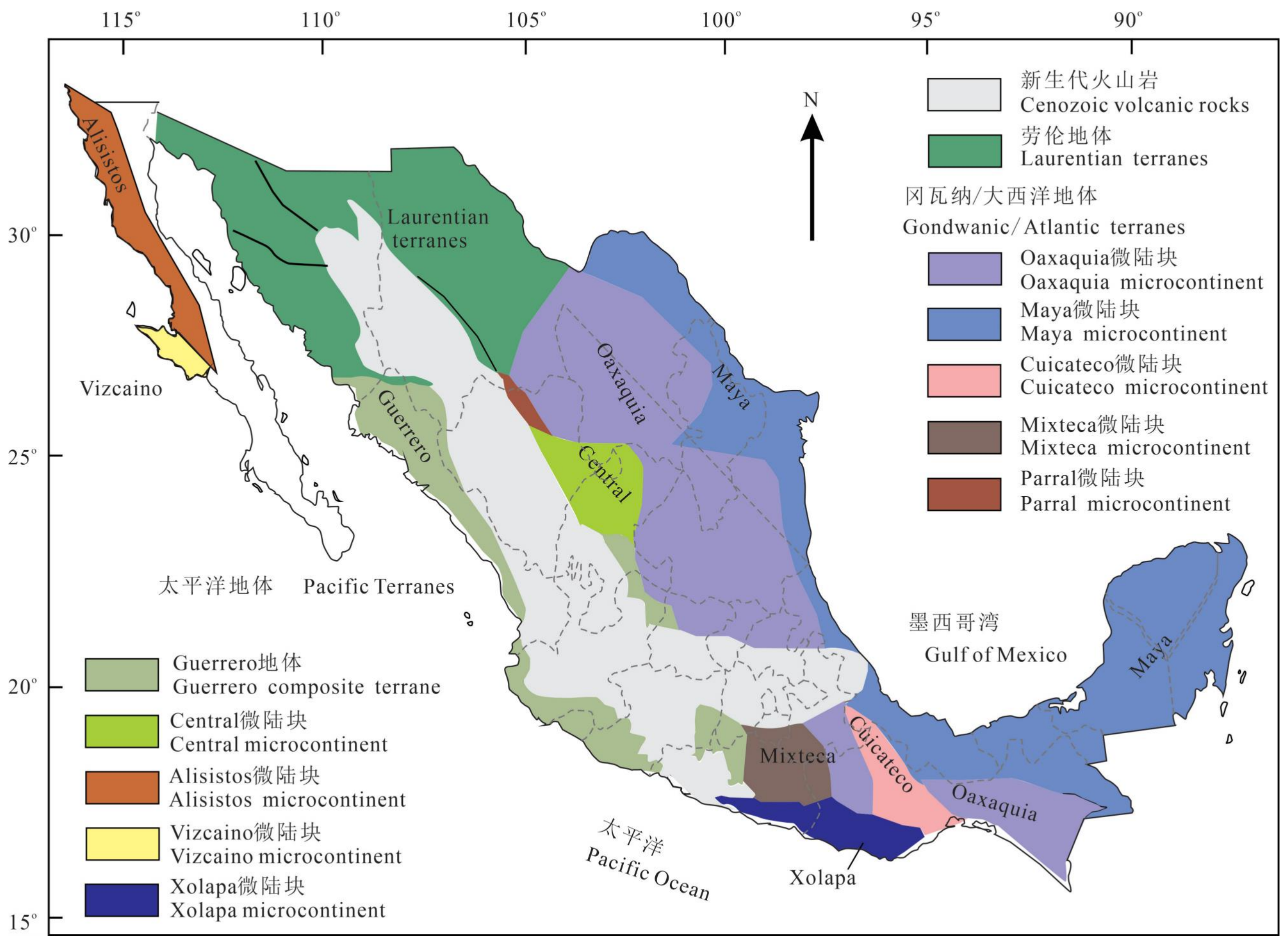

图 1 墨西哥大地构造格架(据 Centeno-Garcia, 2017 修改)
Fig. 1 Tectonostratigraphic terranes of Mexico (modified from Centeno-Garcia, 2017)

用交替进行,岩浆活动和构造增生导致陆壳的加厚。以上两个过程同时作用,造就了墨西哥复杂的地质环境。由于墨西哥构造演化的复杂性,致使现今的墨西哥大陆由多个各具特色的地体拼接而成,这些地体具有不同的构造—地层组合,并且多以大断层为边界(Centeno-Garcia, 2017)。

就大型斑岩铜矿的分布而言,前人研究认为基底物质组成对矿床分布起主要作用(Ortega-Gutiérrez et al., 1995; Talavera-Mendoza et al., 1995; McDowell et al., 1999; Valencia-Moreno et al., 2001; Talavera-Mendoza and Guerrero-Suástegui, 2000)。虽然基底岩石的露头少见并且呈孤立分布,但区域地球化学数据间接表明,墨西哥东部和西北部地区基底是老地壳演化而来。根据酸性火成岩的同位素特征和基底岩石露头分布的主要差异,墨西哥地体在古地理上可以分为 3 大类(图 1)(Centeno-Garcia, 2017;唐伟等,2020):① 劳伦(Laurentian)地体,具有前寒武纪基底,并/或在其年轻的火成岩岩石同位素组成中可见老地壳特征;② 冈瓦纳(Gondwanic)地体/大西洋(Atlantic)地体,包含前寒武纪高级变质基底或下中古生界变质基底(主要是片岩混杂体);③ 太平洋地体,其中最古老的岩石年龄是晚古生代到中生代,并/或含有具有年轻同位素特征的火成岩和变质岩。

劳伦地体被认为与北美克拉通南部元古代地质演化有关,主要出露在墨西哥西北部。墨西哥大部分构造演化与岩浆作用有关,但这种岩浆活动的物质成分,区域分布,体积和大地构造环境等方面在整个中生代都经历了的重大变化。伴随伸展和收缩变形事件发生,引起主要区域地层的不整合关系(Centeno-Garcia, 2017)。

2　墨西哥北部拉拉米期构造岩浆演化

墨西哥北部是记录北美科迪勒拉构造事件最为

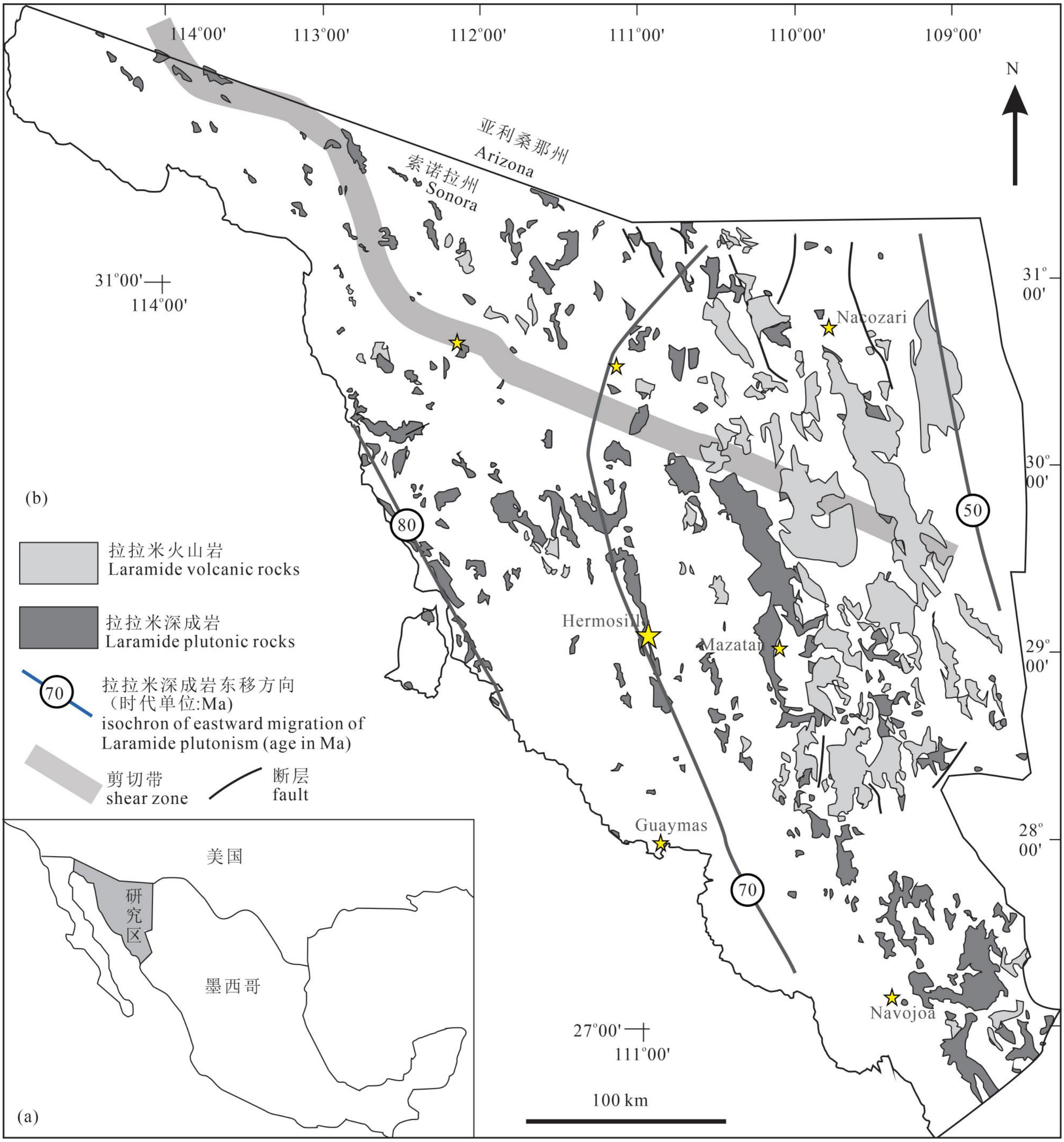

图 2 墨西哥索诺拉地区拉拉米期深成岩和火山岩分布图（据 Gonzalez-Leon et al.，2011 修改）
Fig. 2 Outcrop distribution of plutonic and volcanic rocks of the Laramide magmatic arc in Sonora, Mexico (modified from Gonzalez-Leon et al.，2011)

重要的地区。中生代，古太平洋板块不断俯冲到北美板块之下。基底为劳伦地体的墨西哥西北部在中生代记录的所有火山活动都与法拉隆（Farallon）板块的俯冲有关。科迪勒拉岩浆作用始于泛大陆解体的二叠纪（275~258 Ma，深成岩锆石 U-Pb）（Arvizu et al.，2009）。晚三叠世至晚侏罗世，以科迪勒拉弧岩浆活动为主，区域分散出露 Elenita 组和 Henrietta 组的深成岩和火山岩（Busby-Spera，1988；Grajales-Nishimura et al.，1992；Rio-Salas et al.，2017）。在 97~59 Ma，由于法拉隆板块向北美板块俯冲角度的减小，岩浆活动中心逐步向东迁移至索罗那州和奇瓦瓦州的交界地带（Coney and

Reynolds, 1977; Ortega-Rivera, 2003; Valencia-Moreno et al., 2006;Rio-Salas et al., 2017)。全球同期构造事件响应的拉拉米造山运动(80~40 Ma)在该区域主要表现为基底抬升和逆冲断层变形的挤压作用,岩浆弧的东移引发科迪勒拉地区发生广泛的岩浆活动和陆壳的增厚(Coney and Reynolds, 1977; Damon et al., 1983; Rio-Salas et al., 2017)。呈北西—南东向的构造走向的科迪勒拉岩浆带在索诺拉州和亚利桑那州广泛分布,但在墨西哥西部和南部逐渐减少。在始新世早期和中期,索诺拉州的岩浆活动处于平静期。随着新生代西马德雷大火成岩省的形成(约 38 Ma)(Ferrari et al., 2002, 2018),岩浆活动开始活跃。在 25~12 Ma,火山作用与形成盆岭地貌的拉张构造运动同时发生(Ferrari et al., 2018)。盆岭地貌的走向为 NW—SE,发育 N—S 向正断层。

拉拉米岩浆弧在墨西哥北部分布广泛(图 2)。晚白垩世,俯冲作用引发的火山作用形成了拉拉米期闪长岩—二长花岗岩组成的深成岩及塔拉乌马拉(Tarhumara)组安山岩、流纹岩和凝灰岩火山岩系,后期被古新世—始新世拉拉米花岗闪长岩侵入(McDowell et al., 2001; Valencia-Moreno and Ortega-Rivera, 2011)。该套花岗闪长岩和斑岩侵入岩的热液来源一致,花岗闪长岩体被认为是斑岩型铜钼矿化分异的母岩深成体(Precursor plutonic body)(Noury and Calmus, 2021)。拉拉米岩浆弧是建立在 Caborca 地块和 Mazatzal 地块两个不同的结晶基底之上(Gonzalez-Leon et al., 2011)。拉拉米期塔拉乌马拉(Tarhumara)组火山岩与下伏地层不整合接触关系表明该期岩浆弧主要作用在构造增厚的地壳上(Gonzalez-Leon et al., 2011)。

在拉拉米构造运动期间,岩浆中心自索诺拉州向东持续迁移,在 30 Ma 时限内有 3 次岩浆活动高峰期,分别为 76~70 Ma, 63~57 Ma 和 46~40 Ma(图 3)(Young et al., 2000; Mizer et al., 2015; Rioux et al., 2016; Amato et al., 2017)。40 Ma 之后随着拉拉米构造运动的减弱,岩浆活动减弱。

3 墨西哥北部斑岩型铜矿分布特征

墨西哥斑岩铜矿床由北至南呈连续带状分布,这个带从北部索诺拉州向南延伸到锡那罗亚州南部,主体分布在区域大的近北西/南东向剪切带南北两侧(图 4)。卡纳内亚(Cananea)成矿区的 Buenavista del Cobre 矿床和 Nacozari 成矿区的 La

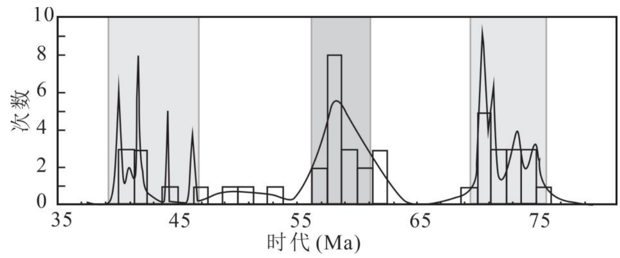

图 3 墨西哥北部拉拉米期岩浆活动频次图(数据来源: Young et al., 2000; Mizer et al., 2015; Rioux et al., 2016; Amato et al., 2017)

Fig. 3 Frequency diagram of Laramide magmatic activity in northern Mexico(modified from Young et al., 2000; Mizer et al., 2015; Rioux et al., 2016; Amato et al., 2017)

Cariad 矿床是墨西哥规模最大的两个斑岩型铜矿床。

对区内早期深成岩与成矿岩体的同位素测年结果显示,El Pilar、La Caridad 和 Suaqui Verde 矿床的早期侵入岩年龄与矿化年龄时间跨度相差较小,为 2 Ma,而少数矿床如 Buenavista del Cobre 矿床 2 个事件的时间跨度相对较大,约为 5 Ma,表明斑岩体是在早期深成侵入岩冷却过程中侵位的(Santillana-Villa, 2021)。最新的辉钼矿 Re-Os 同位素研究显示,最早的矿化发生在 73.9 Ma(El Pilar 矿床),其次为 63.1~63 Ma(Milpillas 矿床)、61.8 ~ 61.6 Ma(Lucy 矿床)、60.4 Ma(Maria 矿床)、60.9 ~ 60.8 Ma(El Alacrán)、59.3 ~ 59.2 Ma(Buenavista del Cobre)和 59.3 ± 0.3 Ma(Mariquita 矿床)。除 El Pilar 矿床外,主要的矿化集中发生在约 4 Ma 的时间窗口内。与矿石相关岩体的 U-Pb 锆石年龄表明整个岩浆活动发生在 77.7~57.8 Ma 之间(Del Rio-Salas et al., 2017)。绢英岩化蚀变带的石英—辉钼矿的 Re-Os 同位素年龄为 57.0 ± 0.3 Ma(Barra et al., 2005)。此外拉拉米深成岩的绢云母蚀变带云母的 K-Ar 年龄为 56.9 ± 1.2 Ma 和 56.7 ± 1.1 Ma(Damon et al., 1983)(表 1)。从已有矿床时代特征来看,墨西哥斑岩铜矿床主要的成矿期为晚白垩世和始新世(74~54 Ma; Valencia-Moreno et al., 2006, 2007)(表 1)。

4 典型矿床

卡纳内亚矿集区和纳科札里(Nacozari)成矿区是墨西哥北部重要 2 大产铜矿集区。卡纳内亚矿集区地质上位于科迪勒拉造山带南部,地理上位于索诺拉州北部,与美国接壤边界以南 37 km 处,主要铜

表 1 墨西哥北部斑岩型铜矿成矿时代

Table 1 Metallogenic age of porphyry copper deposits in northern Mexico

序号	矿床名称	所处州	年龄(Ma)	测年方法	矿石量和矿石品位	参考文献
1	Fortuna del Cobre	索诺拉州	74.6 ± 1.3 75.0 ± 1.4	Re-Os	20 Mt@0.5% Cu,0.026% Mo 11 Mt@1.15% Cu (表生)	Salvatierra-Domínguez, 2000; Barra and Valencia, 2014
2	Los HuMos	索诺拉州	73.5 ± 0.2	Re-Os	300 Mt @0.3% Cu	Barra and Valencia, 2014
3	El Pilar	索诺拉州	73.9 ± 0.3	Re-Os	259 Mt @ 0.3% Cu	Del Río-Salas et al. ,2015
4	Milpillas	索诺拉州	63.1 ± 0.4	Re-Os	230 Mt @ 0.85%Cu	Noguez-Alcántara et al. , 2007; Singer et al. , 2008
5	Mariquita	索诺拉州	59.3 ± 0.3	Re-Os	100 Mt@ 0.48% Cu	Aponte-Barrera, 2009; Del Río-Salas et al. , 2015
6	Lucy	索诺拉州	61.6 ± 0.3, 61.8 ±0.3	Re-Os	9 Mt mined @ 0.8% Cu, 0.1% Mo	González-Partida et al. , 2009; Del Río-Salas et al. , 2015
7	María	索诺拉州	60.4 ± 0.3	K-Ar	8.6 Mt@1.7% Cu, 0.01% Mo	Barton et al. , 1995; Barra et al. , 2005; Del Río-Salas et al. , 2015
8	Buenavista del Cobre	索诺拉州	59.3 ± 0.3	Re-Os	7,140 Mt at 0.42% Cu, 0.008% Mo	Barra et al. , 2005; Barton et al. , 1995; Singer et al. , 2008
9	El Alacrán	索诺拉州	60.9 ± 0.2	Re-Os	24 Mt@ 0.35% Cu	Barra et al. , 2005
10	La Caridad	索诺拉州	53.6 ± 0.2 54.0 ± 0.2	Re-Os	1800Mt@ 0.452% Cu, 0.0247% Mo	Barra et al. , 2005; Valencia et al. , 2005; Singer et al. , 2008
11	Pilares	索诺拉州	53.6 ± 1.1	U-Pb	147 Mt @1.04% Cu	Singer et al. , 2008; Gómez-Landa, 2014
12	Florida-Barrigón	索诺拉州	52.4 ± 1.1	K	135 Mt @ 0.33% Cu	Damon et al. , 1983; Valencia et al. , 2006; Singer et al. , 2008
13	CuMobabi	索诺拉州	58.7 ± 0.2	Re-Os	67 Mt @ 0.266% Cu, 0.099% Mo	Barra et al. , 2005; Singer et al. , 2008
14	Washignton	索诺拉州	56.4 ± 1.2	K-Ar	1.2 Mt@ 1.7% Cu, 0.058% Mo	Damon et al. , 1983; Valencia et al. , 2006
15	El Crestón	索诺拉州	53.6 ± 0.2	Re-Os	215.4 Mt @ 0.059% Cu,0.071% Mo	Barra et al. , 2005; Valencia-Moreno et al. , 2006; Singer et al. , 2008
16	San Antonio de la Huerta	索诺拉州	57.4 ± 1.4	K-Ar	3.6 Mt@ 1% Cu	Damon et al. , 1983
17	Suaqui Verde	索诺拉州	57.0 ± 0.3	Re-Os	87.2 Mt @ 0.43% Cu	Barra et al. , 2005; Valencia-Moreno et al. , 2006; Singer et al. , 2008
18	Cuatro Hermanos	索诺拉州	55.7 ± 0.3	Re-Os	233 Mt@ 0.43% Cu, 0.035% Mo	Barra et al. , 2005; Zürcher, 2002; Singer et al. , 2008
19	Santa Rosa	索诺拉州	55.7 ± 0.8	Ar/Ar	1.1 Mt @ 0.524% Cu, 0.121% Mo	Mead et al. , 1988
20	Piedras Verdes	索诺拉州	~ 60.0	Re-Os	452.790 Mt @0.28% Cu	Dreier and Braun, 1995; Espinosa-Perea, 1999
21	Santo Tomás	锡那罗亚州	57.2 ± 1.2	K-Ar	274 Mt @ 0.498% Cu, 0.05 g/t Au	Damon et al. , 1983; Singer et al. , 2008
22	La Reforma	奇瓦瓦州	59.2 ± 1.3	K-Ar	-	Damon et al. , 1983
23	Bahuérachi	奇瓦瓦州	65.7	-	524.5 Mt@ 0.40% Cu, 0.008% Mo	Tyler Resource Inc. , 2008
24	Tameapa	锡那罗亚州	57.0~52.0	Re-Os	54 Mt @ 0.4% Cu	Barton et al. , 1995; Barra et al. , 2005; Singer et al. , 2008
25	Los Chicharrones	锡那罗亚州	56.2 ± 1.2	K-Ar	-	Damon et al. , 1983; Zürcher, 2002
26	Malpica	锡那罗亚州	54.1 ± 0.3	Re-Os	11.14 Mt@ 0.55% Cu (氧化带); 53.88 Mt @0.61% Cu (硫化带)	Barton et al. , 1995;Barra et al. , 2005
27	Las Azulitas	锡那罗亚州	59.5 ± 1.2	K-Ar		Damon et al. , 1983

矿床包括 Buenavista del Cobre 矿床、Milpillas 矿床、Lucy 矿床、Mariquita 矿床、María 矿床、El Alacr'an 矿床、El Pilar 矿床等。Nacozari 成矿区位于 Cananea 矿区东南约 80 km 处的 Nacozari 镇,区内分布的 La Caridad 矿床、Pilares 矿床、Santo Domingo 矿床、Los Alios 矿床、Bella Esperanza 矿床、El Batamote 矿床、Florida-Barrig'on 矿床等。

4.1　Buenavista del Cobre 矿床

Buenavista del Cobre 矿床(简称 BC 矿床)位于墨西哥索诺拉州卡纳内亚成矿区内。主要矿化脉冲

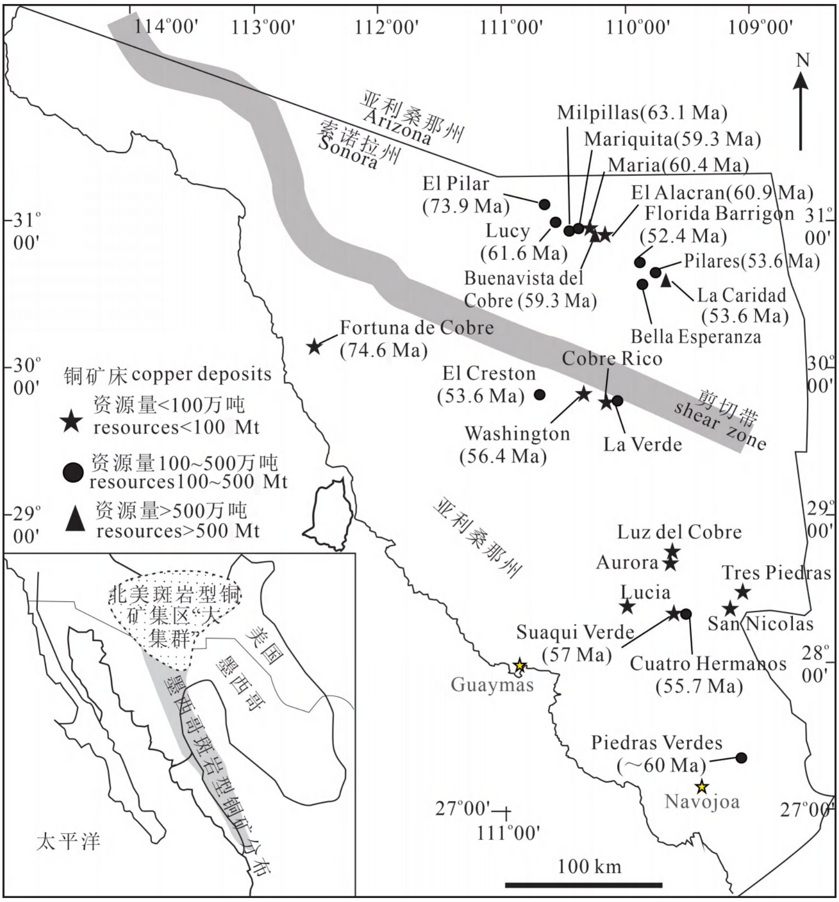

图 4 墨西哥索诺拉地区铜矿床分布图(数据来源表 1)

Fig. 4 Distribution map of copper deposits in Sonora, Mexico (data from Table 1)

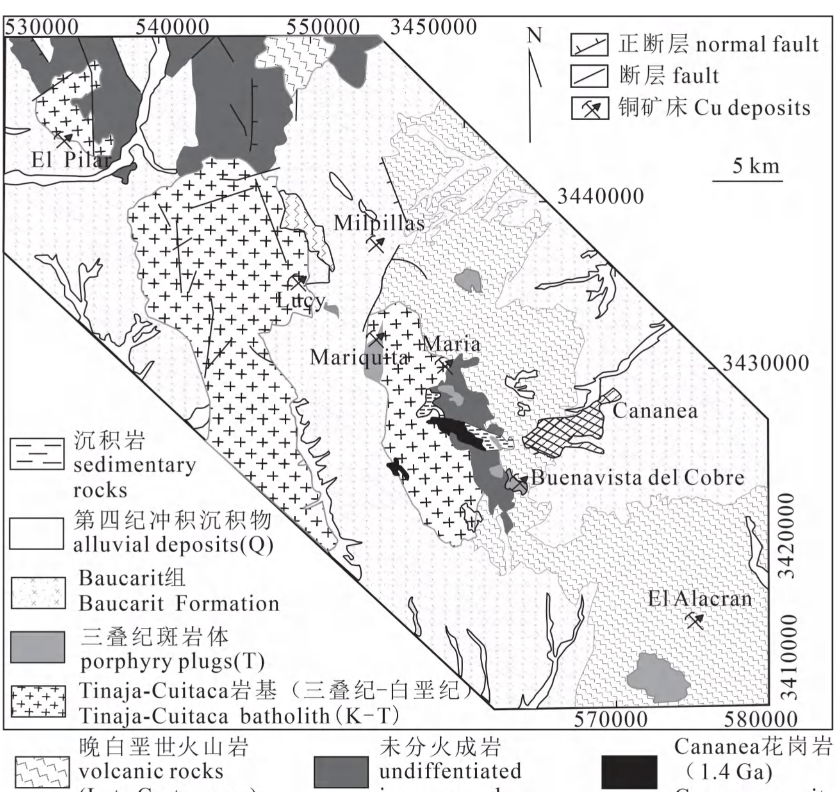

发生在约为 5 Ma 时间窗内。区内变质基底为绢云母片岩(1.7~1.6 Ga, Santillana-Villa, 2021)。后期被 Cananea 花岗岩(1.4 Ga)和 Aib'o 花岗岩的(1.1 Ga)侵入(Anderson and Silver,1977)(图 5)。元古代岩石被一系列由 Bolsa 组、Abrigo 组、Martín 组和 Escabrosa 组以及 Naco 组的碳酸盐岩组成的新元古代和古生代钙质沉积岩覆盖(Meinert, 1982)。后期被三叠纪—侏罗纪埃莱尼塔组(Elenita Formation)和亨丽埃塔组(Henrietta Formation)流纹岩和安山岩火山层序不整合覆盖(Meinert, 1982)。

矿区内基底岩石为 1.4 Ga 花岗岩,古生代的石英岩和灰岩覆于基底之上(Anderson and Silver, 1977)。三叠纪—侏罗纪 Elenita 组和 Henrietta 组的凝灰岩不整合覆于古生代岩石之上(图 6)。拉拉米(Laramide)期 Mariquita 组和 Mesa 组火山岩覆盖三叠纪和侏罗纪火山岩之上(Meinert, 1982; Bushnell, 1988)。Cuitaca (64 ± 3 Ma) 和 Tinaja 深成岩(69 ± 1 Ma)分别侵入侏罗纪火山岩。同时,伴随着大量的斑岩岩株(63.9 ± 1.3 Ma、58.9± 1.4 Ma)侵入侏罗纪火山岩地层内(Valencia et al., 2006; Del Rio-Salas et al., 2015)。区内侵入岩主

图 5 布埃纳维斯塔铜矿床及周边地质图(Santillana-Villa, 2021)

Fig. 5 The geological map of the Buenavista del Cobre copper deposit and the surrounding areas (modified from Santillana-Villa, 2021)

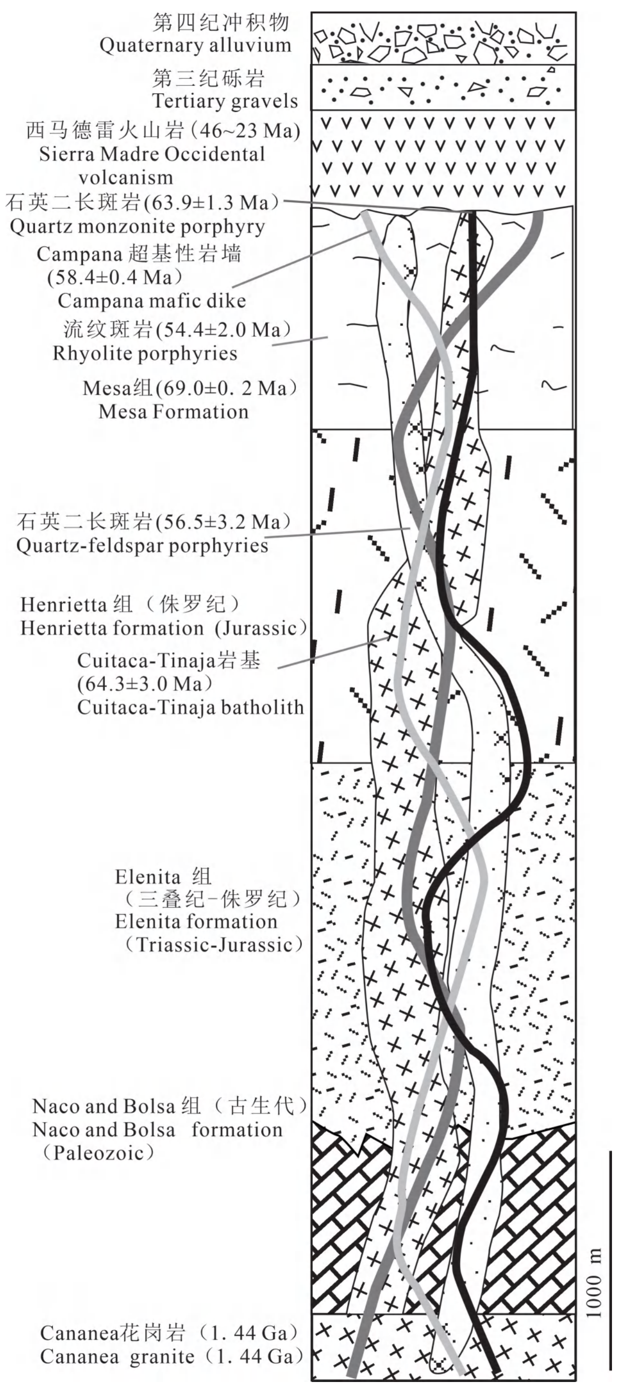

图 6 布埃纳维斯塔铜矿区地层柱状图
(Barra et al., 2005)
Fig. 6 Stratigraphic column of the Buenavista del Cobre copper deposit (modified from Barra et al., 2005)

要为石英二长岩、二长闪长岩和花岗闪长岩。花岗闪长岩为中—粗粒,由斜长石(~40%)、石英(~25%)、钾长石(~15%)、黑云母及角闪石(~15%)和不透明矿物(~5%)组成。富矿的正长岩,斑状结构,主要由钾长石(~40%)、黑云母(~10%)、斜长石(~10%)组成。岩石遭受绢云母化蚀变作用。

该地区的构造演化在矿床形成后仍在继续。在渐新世和中新世时期,发生了强烈的断层、伸展、旋转等构造作用,旋转幅度从中等(30° ~ 60°)到强烈(60° ~ 90°)不等(Wilkins and Heinrich,1995)。使得矿体遭到不同程度的破坏。区域影响矿床展布的构造主要分为两种,分别为与成矿有关的北东向构造和成矿后期的北西向构造。

浸染状和网脉状矿化主要发生在 Henrietta 组和 Mesa 组火成岩内,石英长石斑岩是主要的赋矿岩体,围岩为区内广泛出露的 Cuitaca 花岗闪长岩(64 Ma)。矿石辉钼矿的 Re-Os 同位素年龄为(59.3~59.2) ± 0.3 Ma(Del Rio-Salas et al., 2017)。强烈的构造作用使斑岩侵入体周围发育网脉状带。斑岩侵位伴随着强烈的热液作用,蚀变以钾化和石英—绢云母蚀变为主(Ochoa-Landín and Echavarri, 1978)。

4.2 El Pilar 矿床

El Pilar 矿床位于卡纳内亚矿集区的西北部,巴塔哥尼亚山脉(Patagonia)的西南侧。古生代沉积岩覆盖在前寒武侵入岩之上,古近纪沉积岩覆在古生代地层之上,被后期花岗岩类侵入岩侵入(图 7)。古近纪和第四纪冲积扇和冲积沉积盖层分布在山脉的两侧和中间的谷地(Santillana-Villa et al., 2021)。该矿床发育两个阶段的矿化,第一阶段矿化发生在 73.9 ± 0.3 Ma(辉钼矿 Re-Os 年龄)(Del Rio-Salas et al., 2017)。与矿化时代相近的花岗闪长岩侵入岩时代为 74.6 Ma,矿化作用在空间上与二长岩到石英二长岩的 El Pilar 岩体有关(Broch, 2012;Del Rio-Salas et al., 2017);第二阶段矿化发生在中新世期间,主要为原生矿化受后期构造影响和侵蚀后铜的再活化和再富集。

El Pilar 铜矿床 N33E 长约 2300 m,宽 600~1000 m,NW—SE 平均厚度 110 m(范围 5~220 m)。El Pilar 大约 98% 的铜赋存在松散的、分选差、弱固结、角砾为花岗岩、斑岩及高度硅化岩石碎屑的沉角砾岩内。矿化的沉角砾岩被第四纪冲积扇沉积物覆盖。铜矿化主要为以涂层的形式出现在高度硅化碎屑岩上及沉积角砾岩基质内的孔雀石矿化。其他含铜矿物包括黄铜矿、斑铜矿、铜蓝矿、蓝铜矿、孔雀石、和紫铜矿等。区内无相关蚀变信息报道,但是角砾岩的部分碎屑有高度硅化现象。El Pilar 铜矿床有一个明确的金属分区,高品位铜赋存在角砾岩内,从矿床的核心向外,铜品位逐渐降低(Broch, 2012)

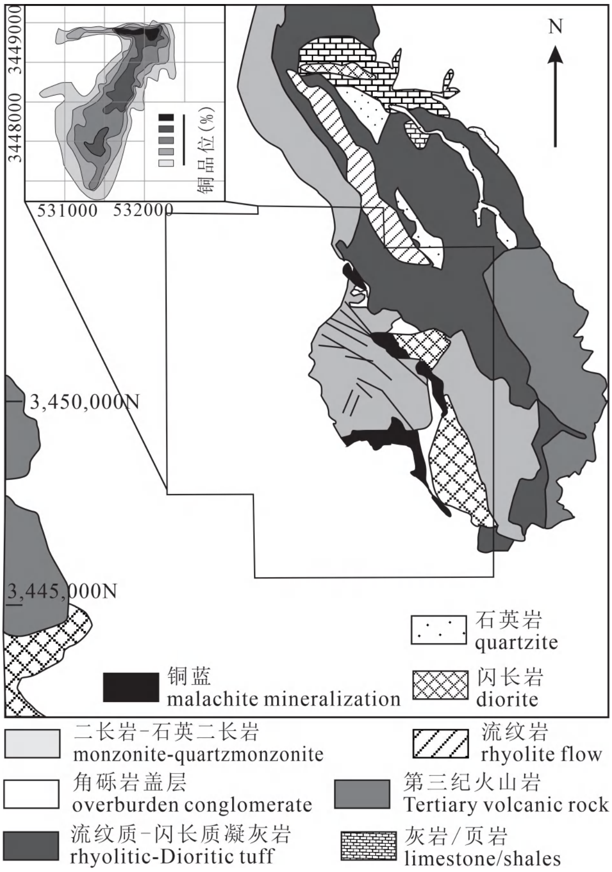

图 7 El Pilar 铜矿床矿区地质图(据 Broch, 2012)

Fig. 7 Geological map of the El Pilar copper deposit (modified from Broch, 2012)

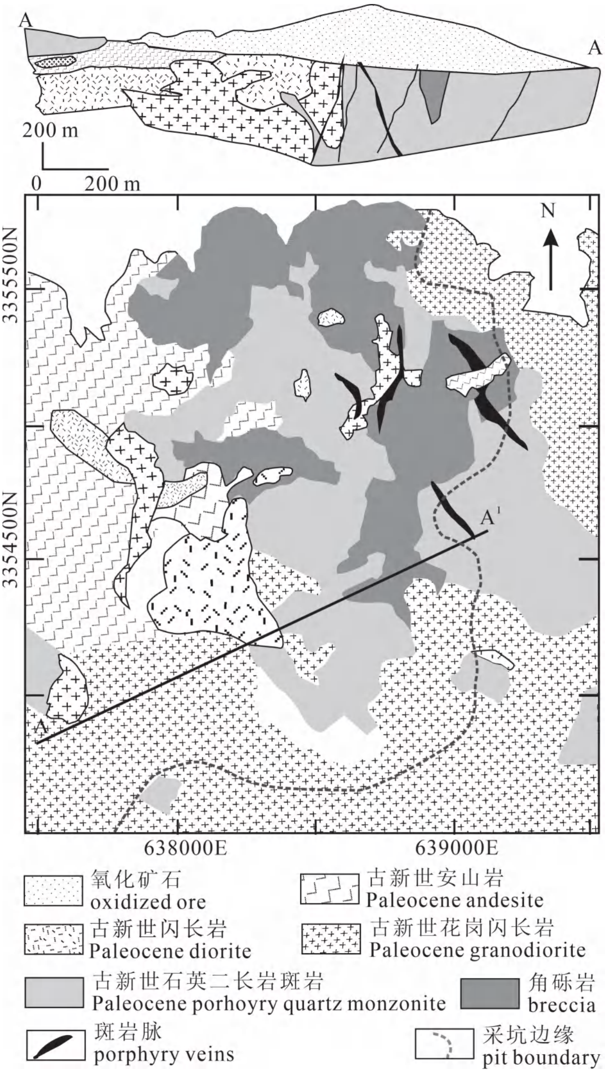

图 8 La Caridad 铜矿床地质图(据 Valencia, 2008)

Fig. 8 Geological map of the La Caridad copper deposit (from Valencia, 2008)

(图 7)。

4.3 La Caridad 铜矿床

La Caridad 矿位于 Nacozari 成矿区东南约 14 km 处(图 8)(Singer et al., 2008)。矿化主要发生在 Tarahumara 组的火山岩中,硫化物矿物主要呈浸染状和网脉状产出,局部赋存在角砾岩和伟晶岩内。矿化作用与区内约 55.5 Ma 的最早的花岗闪长岩的侵入有关,石英二长斑岩是主要的成矿岩体,矿化年龄为 54.3 ± 1.7 Ma(Valencia et al., 2005)。

由于法拉隆板块的俯冲引发的钙碱性岩浆作用,La Caridad 地区的变质基底被中侏罗世由火山碎屑、砂岩和凝灰岩组成的砾岩以及 Lily 组和 Coppercuin 组的湖相灰岩不整合覆盖(McAnulty, 1970)。

La Caridad 地区北东向的正断层抑制了下盘拉拉米期花岗闪长岩的剥蚀,对上盘 La Caridad Vieja 热液矿床起到了很好的保护作用(Valencia et al., 2008;Berrajano-Carillo et al., 2020)。花岗闪长岩侵入岩的锆石 U-Pb 年龄为 58.3 ± 2.0 Ma 和 53.3 ± 1.6 Ma(Valencia et al., 2005; Gonz'alez Le'on et al., 2017);斑岩的结晶年龄为 55.0 ± 1.7 Ma 和 52.6 ± 1.6 Ma(Valencia et al., 2005, 锆石 U-Pb 年龄)。辉钼矿的 Re-Os 同位素矿化时代为 53.8 ± 0.2 Ma 和 53.6 ± 0.2 Ma(Barra et al., 2005)。花岗岩闪长岩侵入年龄、斑岩结晶年龄和辉钼矿的 Re-Os 同位素年龄几乎同期,说明 La Caridad 岩体是一个复合侵入岩体,侵位时限至少经历了 6 Ma。La Caridad 矿床花岗闪长岩和斑岩的磷灰石 U-Pb 年龄分别为 64.1 ± 9.8 Ma 和 52.9 ± 1.4 Ma(Valencia et al., 2005)。52.6 ± 1.6 Ma 的岩浆活动是区内最后一期岩浆活动,花岗闪长岩和斑岩侵入体经历了同期的热演化作用(Valencia et al., 2005)。

在强烈的构造作用下,区内岩石破碎严重,裂隙发育。裂隙大大提高了围岩的渗透性,是影响整个矿床表生矿化分布的重要因素。区内断裂方向一般呈北东、北西和东西走向,其中北东方向断裂作用最强。在矿床中部的北东走向的山脊上强烈蚀变和矿化作用与山脊走向一致。斑岩侵入体的北西向延伸表明北西向断裂构造影响了这些侵入体的就位。

La Caridad 矿床的蚀变和矿化在空间上是同时存在的,并且似乎是同时期的。蚀变具明显的分带现象,内部主要为绢云母和泥化蚀变,外带为与围岩接触部位发生青磐岩化蚀变。

与热液蚀变同时形成的深成硫化矿化作用形成的矿石矿物按丰度递减顺序包括黄铁矿、黄铜矿、辉钼矿、闪锌矿、方铅矿和非常稀有的斑铜矿。硫化物矿物以裂缝填充物、浸染状和角砾岩基质置换的形式出现。在矿床的中部,约 60% 的黄铜矿和黄铁矿以浸染状的形式出现,其余的则以细脉和晶体聚集体的形式填充角砾岩空腔。黄铜矿含量从矿床中心向外逐渐减少,然后在边缘附近急剧减少,而边缘区的黄铁矿含量与中心区大致相同。

5　讨论

5.1　斑岩型铜矿床时空分布与拉拉米岩浆活动的耦合关系

墨西哥包括 BC 斑岩型铜矿床沿着 NW—SE 走向的拉拉米(Laramide)岩浆弧分布,在弧的西部,斑岩型铜矿较少,铜矿化多数形成于岩浆弧东移期间(图 9)。拉拉米期,法拉隆板块向北美板块俯冲,板块俯冲角度逐渐减小致使地壳增厚并伴随着岩浆活动中心逐步向东迁移(Valencia - Moreno et al., 2006;图 9)。俯冲作用促使地幔楔的部分熔融,软流圈岩浆沿着断裂上涌至熔融区,不仅提供了形成火成深成混合岩所需的钙碱性岩浆,而且为大量世界级岩浆热液型铜钼等相关的矿化提供了环境(图 10)。从某种程度上可以说明,区内拉拉米(Laramide)造山作用是形成区内巨量铜钼富集的主要地质作用(Saleeby, 2003; English and Johnston, 2004)。

在 75~52 Ma 之间,大约 23 Ma 相对较短的时间范围内,在拉拉米岩浆弧带分布了众多巨量的斑岩型矿床,资源量超过 800 万吨的铜矿床出现在 14 Ma 时间范围较短的区域(多集中在 69~54 Ma),而其他超大型(资源量大于 2500 万吨铜)的斑岩型铜矿床如 Buenavista del Cobre 矿床则集中出现在更短的 7 Ma 时间范围内(多集中在 63~56 Ma)(图 11)。因此可以推测,墨西哥北部整个拉拉米岩浆弧内约 60%的斑岩型铜矿的成矿作用集中发生在 63~56 Ma,时间跨度约为 7 Ma。

5.2　斑岩型铜矿床特征及控矿因素

由于受到中新世盆岭拉张构造作用的破坏,墨西哥北部斑岩型铜矿的矿化系统的原始特征很难重构,本文试图从典型 Buenavista del Cobre 矿床、La Caridad 矿床和 El Pilar 典型矿床入手,梳理成矿特

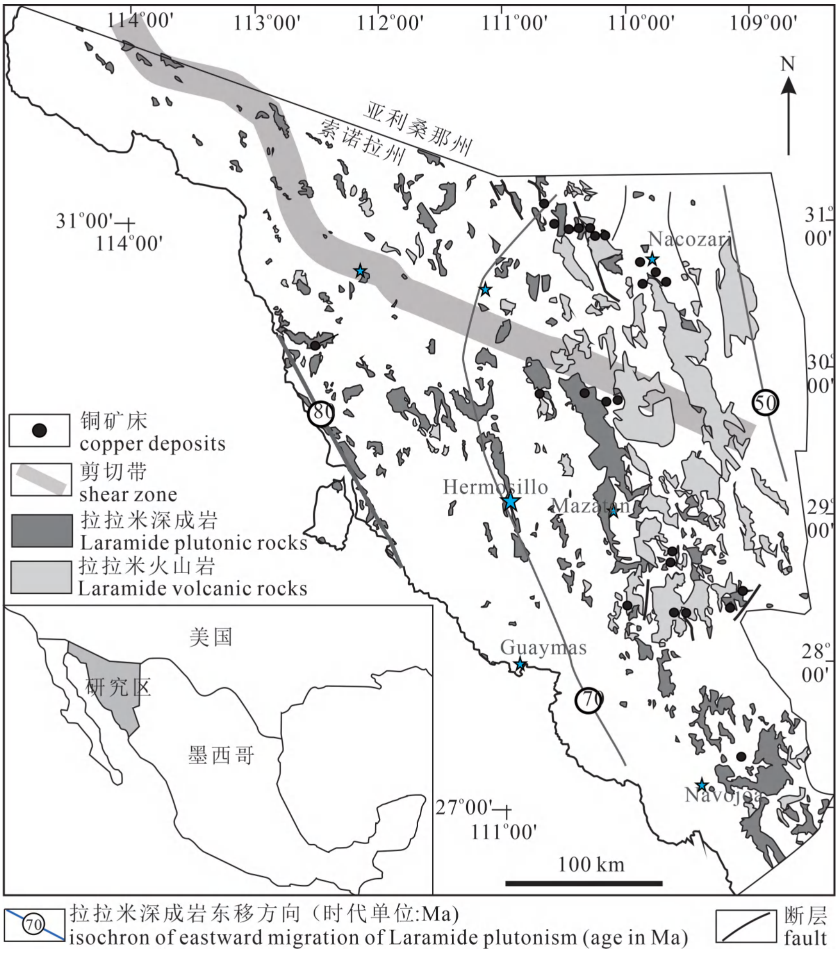

图 9 墨西哥索诺拉地区拉拉米期岩浆弧与斑岩型铜矿耦合关系图

Fig. 9 Coupling map of Laramide magmatic arc and porphyry copper deposits in Sonora, Mexico

表 2 拉拉米期斑岩型铜矿床成矿特征表

Table 2 Metallogenic characteristics of Laramide porphyry copper deposits

矿床名称	El Pilar 矿床	Buenavista del Cobre 矿床	La Caridad 矿床
成矿时代	73.9±0.3 Ma	59.3±0.3 Ma	53.6±0.2 Ma
矿石矿物	黄铜矿、斑铜矿、铜蓝矿、蓝铜矿、孔雀石和紫铜矿	黄铁矿、黄铜矿、辉铜矿、铜蓝、辉钼矿	黄铁矿、黄铜矿、辉铜矿、闪锌矿、方铅矿、铜蓝、辉钼矿、黝铜矿
侵入岩	花岗闪长岩	石英二长岩、二长闪长岩和花岗闪长岩	花岗闪长岩
矿化特征	孔雀石、角砾岩	脉状—网脉状、浸染状、角砾岩	脉状—网脉状、浸染状、角砾岩
蚀变类型	硅化	钾化和绢云母蚀变	蚀变具明显的分带现象,内部主要为绢云母和泥化蚀变,外带为与围岩接触部位发生青磐岩化蚀变。
赋矿岩石	石英长石斑岩、角砾岩	石英长石斑岩	石英二长斑岩、伟晶岩、角砾岩
构造特征	构造强烈,断裂发育	构造强烈,裂隙发育	构造强烈,裂隙发育

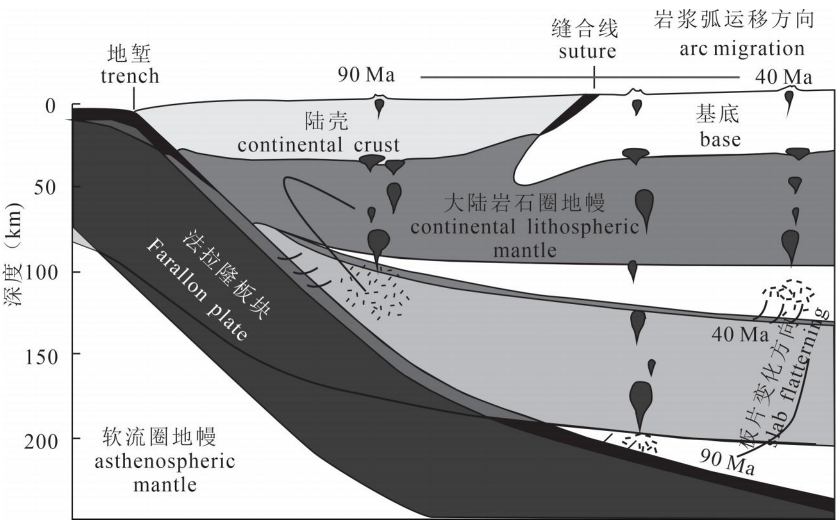

图 10 早白垩世到始新世岩石圈截面图,俯冲板片的逐渐变平导致岩浆弧向东迁移(据 Valencia-Moreno et al., 2021 修改)

Fig. 10 Lithosphere cross-section from Early Cretaceous to Eocene, the progressive flattening of the subducted slab caused the migration of the magmatic arc to the east (modified from Valencia-Moreno et al., 2021)

征,总结控矿因素(表 2)。

墨西哥北部斑岩型铜矿床主要成矿时代为拉拉米期,铜矿床的分布沿着拉拉米岩浆弧展布,矿床在时间上与侵入岩有关,成矿高峰期内的矿床矿石矿物组合类似,具明显的绢云母等蚀变特征,发育众多的小断距断层及断裂带。同时,始新世—渐新世的火山岩(厚度<500 m)对矿床免受剥蚀起到了一定的保护作用。该区域的斑岩铜矿呈表生富集的特征。新生代的断层构造在墨西哥西北部对斑岩型铜的保存与侵蚀发挥了巨大作用(Barton et al., 1995)。索诺拉州的伸展构造,特别是在卡纳内亚矿区,可能已经切割和掩埋了部分斑岩铜系统。

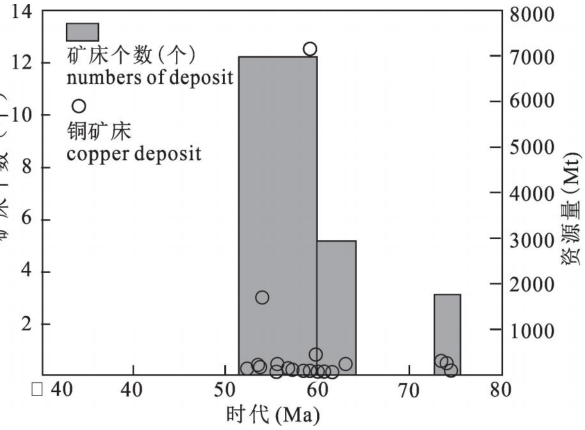

图 11 墨西哥索诺拉拉拉米期斑岩铜矿床资源量与成矿年龄关系图(数据来源表 1)

Fig. 11 Diagram of copper contained versus metallogenic age from Laramide porphyry copper deposits of Sonora (data from Table 1)

6 结论

(1)墨西哥北部是墨西哥铜资源最为丰富的地区,以斑岩型成矿类型为主,成矿时代主要集中在晚白垩世—始新世。铜的成矿和富集与拉拉米期运动有关。

(2)墨西哥北部斑岩型铜矿床,矿化与花岗闪长岩侵入有关,呈浸染状和网脉状矿化特征,矿石主要赋存在石英长石斑岩内,以钾化和石英—绢云母蚀变为主要蚀变类型,高品位矿石均经历表生富集作用。

参 考 文 献 / References

(The literature whose publishing year followed by a "&" is in Chinese with English abstract; The literature whose publishing year followed by a "#" is in Chinese without English abstract)

唐伟, 汤正江, 程治民, 高鹏, 王秋璇. 2020. 水系沉积物地球化学测量在墨西哥 Tomatlan 地区铜矿预查中的应用. 华东地质, 41(2): 159~165. 杨超, 陈星辉, 赵晓波. 2020. 斑岩铜矿研究进展兼论中国斑岩铜矿勘查现状及潜力. 陕西地质, 38(2): 25~38.

杨志明, 侯增谦, 周利敏, 周怿惟. 2020. 中国斑岩铜矿床中的主要关键矿产. 科学通报, 65(33): 3653~3664.

Amato J M, Mach G H, Jonell T N, Seager W R, Upchurch G R. 2017. Onset of the Laramide orogeny and associated magmatism in southern New Mexico based on U-Pb geochronology. The Geological Society of America Bulletin, 129(9~10): 1209~1226.

Anderson T H, Silver L T. 1977. U-Pb isotope ages of granitic plutons near Cananea, Sonora. Economical Geology, 72: 827~836.

Aponte-Barrera M. 2009. Geología y mineralización del yacimiento Mariquita, distrito de Cananea. In: Clark K F, Salas-Pizá G, Cubillas-Estrada R. ed. Geología económica de México. 2nd edición Servicio Geológico Mexicano-Asociación de Ingenieros de Minas, Metalurgista Cs y Geólogos de México, 852~856.

Arvizu E H, Iriondo A, Izaguirre A, Ch'avez-Cabello G, Kamenov G D, Solis- Pichardo G, Foster D A, Lozano-Santa Cruz R. 2009. Rocas graniticas p'ermicas en la Sierra Pinta, NW de Sonora, M'exico: Magmatismo de subduccion asociadoial inicio del margen continental activo del SW de Norteamerica. Review of Mexico Ciencias Geology, 26: 709~728.

Barra F, Ruiz, J, Valencia V A, Ochoa Landín L, Chesley J T, Zurcher L. 2005. Laramide porphyry Cu-Mo mineralization in northern Mexico: age constraints from Re-Os geochronology in molybdenite. Economic Geology, 100 (8): 1605~1616.

Barra F, Valencia V. 2014. Late Cretaceous porphyry copper mineralization in Sonora, Mexico: implications for the evolution of the southwestern North America porphyry copper province. Mineral Deposita, 49 (7): 879~884.

Barton M D, Staude J M, Zürcher L, Megaw P K M. 1995. Porphyry copper and other intrusion-related mineralization in Mexico. In: Pierc F W, Bolm J G, ed. Porphyry Copper Deposits of the American Cordillera. Arizona Geological Society Digest, 20: 487~524.

Berrajano-Carillo C, Ochoa-Landin L, Rio-Salas R, Valencia-Moreno M, Paez-Beltran C, Ruiz J, Espinoza-Maldonado I. 2020. La Caridad Vieja: Vestiges of a removed HS-epithermal system in the La caridad porphyry Cu-Mo system, northeastern sonora, Mexico, based on XRD, SEM, SWIR spectral analysis and U-Pb zircon dating. Journal of South American Earth Sciences, 104: 102~820.

Bushnell S E. 1988. Mineralization at Cananea, Sonora, Mexico, and paragenesis and zoning of breccia pipes in quartzo feld spathic rock. Economic Geology, 83: 1760~1781.

Broch M. 2012. El Pilar Project, N143-101F1. Technical Report, Feasibility Study. Mercator Minerals Ltd. 302.

Centeno-Garcia E. 2017. Mesozoic tectono-magmatic evolution of Mexico: An overview. Ore Geology Reviews, 81: 1035~1052.

Cooke D R, Hollings P, Walshe J L. 2005. Giant porphyry deposits: characteristics, distribution, and tectonic controls. Economic Geology, 100: 801~818.

Coney P J, Reynolds S J. 1977. Cordilleran benioff zones. Nature, 270: 403~406.

Damon P E, Shafiqullah M, Clark K F. 1983. Geochronology of the porphyry copper deposits and related mineralization of Mexico. Canada Journal of Earth Science, 20: 1052~1071.

Del Rio-Salas R, Ochoa-Landin L, Valencia-Moreno M, Calmus T, Meza-Figueroa D, Salgado-Souto S, Kirk J, Ruiz J, Mendivil-Quijada H. 2017. New U-Pb and Re-Os geochronology of Laramide porphyry copper mineralization along the Cananea lineament, northeastern Sonora, Mexico: Contribution to the understanding of the Cananea copper district. Ore Geology Reviews, 81: 1125~1136.

Del Rio-Salas R, Ochoa-Landín L, Valencia-Moreno M, Calmus T, Meza-Figueroa D, Salgado-Souto S, Kirk J, Ruiz J, Mendívil-Quijada H. 2015. New U-Pb and Re-Os geochronology of Laramide porphyry copper mineralization along the Cananea lineament, northeastern Sonora, Mexico: Contribution to the understanding of the Cananea copper district. Ore Geology Reviews, 81: 1125~1136.

Dreier J E, Braun E R. 1995. Piedras Verdes, Sonora, Mexico: a structurally controlled porphyry copper deposit. In: Pierce F W, Bolm J G, ed. Porphyry copper deposits of the American Cordillera [C]. Arizona Geological Society, 20: 535~543.

English J M, Johnston S T. 2004. The Laramide Orogeny: what were the driving forces? International Geology Review, 46: 833~838.

Espinosa-Perea V. 1999. Magmatic evolution and geochemistry of the Piedras Verdes deposit, Sonora, México. Unpub. M. S. Thesis, The University of Arizona, Tucson, Arizona, USA, 114.

Ferrari L, L'opez Martínez M, Rosas Elguera J. 2002. Ignimbrite flare-up and deformation in the southern Sierra Madre Occidental, western Mexico: implications for the late subduction history of the Farallon plate. Tectonics, 21 (4): 17~1.

Ferrari L, Orozco Esquivel T, Bryan S E, L'opez Martínez M, Silva Fragoso A. 2018. Cenozoic magmatism and extension in western Mexico: linking the Sierra Madre Occidental silicic large igneous province and the Comondú Group with the Gulf of California rift. Earth Science Reviews, 183: 115~152.

Gómez-Landa J R. 2014. Caracterización geológica, estructural, geoquímica y metalogenética de la brecha Pilares, Sonora, México. Unpub. M. S. Thesis, Universidad de Sonora, 86.

Gonz'alez-Le'on C M, Solari L, Valencia-Moreno M, Rasc'on-Heimpel M A, Sol'e J. 2017. Early Eocene magmatic evolution of the Laramide arc in the Nacozari quadrangle, northeastern Sonora, Mexico and its regional implications. Ore Geological Reviews, 81: 1137~1157.

Gonz'alez-Le'on C M, Solari L, Solari L, Sole J, Ducea M N, Lawton T F, Bernal J P, Gonzalez-Becuar E, Gray F, Martinez M L, Santacruz R L. 2011. Stratigraphy, geochronology, and geochemistry of the Laramide magmatic arc in north-central Sonora, Mexico. Geosphere, 7: 1392~1418.

Gonzúlez-Partida E, Pérez-Segura E, Camprubi A, Lhomme T. 2009. Ore-forming fluids in the Lucy porphyry Cu-Mo deposit and its regional significance in the Cananea district (Sonora, Mexico). Journal of Geochemical Exploration, 101: 39.

Grajales-Nishimura J M, Terrell D J, Damon P E. 1992. Evidencias de la prolongacion del arco magmatico Cordillerano del Triasico Tardio-Jurúsico en Chihuahua, Durango y Coahuila. Boletin de la Sociedad Geologica Mexicana, 42: 1~18.

Hou Zengqian, Ma Hongwen, Zaw K, Zhang Yuqun, Wang Mingjie, Wang Zeng, Pan Guitang, Tang Renli. 2003. The Himalayan Yulong porphyry copper belt: Product of large-scale strike-slip faulting in eastern Tibet. Economic Geology, 98: 125~145.

Keith S B, Swan M M. 1995. The great Laramide porphyry copper cluster of Arizona, Sonora and New Mexico: the tectonic setting, petrology and genesis of the world class metal cluster. In: Geology and Ore Deposits of the American Cordillera, Geology Society of Nevada Symposium: 1667~1747.

McAnulty W N. 1970. Geology of the Northern Nacozari District, Sonora, Mexico: New Mexico. Ph. D. thesis. University of New Mexico, 103.

McDowell F W, Housh T B, Wark D A. 1999. Nature of the crust beneath west-central Chihuahua, Mexico, based upon Sr, Nd, and Pb isotopic com - positions at the Tomochic volcanic center. Geological Society of America Bulletin, 111: 823~830.

McDowell F W, Rold'an-Quintana J, Connelly J N. 2001. Duration of Late Cretaceous- Early Tertiary Magmatism in East-Central Sonora, Mexico. Geological Society of America Bulletin, 113: 521~531.

Mead R D, Kesler S E, Foland K A, Jones L M. 1988. Relationship of Sonoran tungsten mineralization to the metallogenic evolution of Mexico. Economic Geology, 83: 1943~1965.

Meinert L D. 1982. Skarn, manto, and breccia pipe formation in sedimentary rocks of the Cananea mining district, Sonora, Mexico. Economic Geology, 77: 919~919.

Mizer J D, Barton M D, and Stegen R. 2015. U-Pb geo-chronology of Laramide magmatism related to Cu-, Zn-, and Fe-mineralized systems, Central Mining Dis-trict, New Mexico. In: Pennell W M, and Garside L J, ed, Proceedings of the Geological Society of Nevada Symposium-New Concepts and Discoveries: Reno, Nevada, Geological Society of Nevada, 2: 1109~1129.

Mutschler F E, Ludington S, Bookstrom A A. 2000. Giant porphyry-related metal camps of the world-A database. Open-File Report, 99~556, online version1. 0. U. S. Geological Survey.

Noury M, Calmus T. 2021. Exhumation history of the La Caridad and Suaqui Verde porphyry copper deposits in the eastern Basin and Range province of Sonora: Insights from thermobarometry and apatite thermochronology. Journal of South American Earth Sciencs, 105: 1~18.

Noguez-Alcántara B, Valencia-Moreno M, Roldán-Quintana J, Calmus T. 2007. Enriquecimiento supergénico y análisis de balance de masa en el yacimiento de pórfido cuprífero Milpillas, Distrito Cananea, Sonora. Revista Mexicana De Ciencias Geologicas, 24: 368~388.

Ochoa-Landín L, Echavarri A. 1978. Observaciones preliminares sobre la secuencia de las intrusiones hipabisales en el tajo Colorado-Veta del Distrito Minero de Cananea. Boletín del Departamento de Geología de la Universidad de Sonora, 1: 57~60.

Ortega-Gutiérrez F, Ruiz J, Centeno-García E. 1995. Oaxaquia, a Proterozoic microcontinent accrected to North America during the late Paleozoic. Geology, 23: 1127~1130.

Ortega-Rivera A. 2003. Geochronological constraints on the tectonic history of the Peninsular Ranges Batholith of Alta and Baja California -tectonic implications for western Mexico. In: Johnson S E, Paterson S R, Fletcher J M, Girty G H, Kimbrough D L, Martín-Barajas A, ed, Tectonic Evolution of Northwestern Mexico and the Southwestern USA. Geology Society Special Paper, 374: 297~335.

Richards J P. 2009. Postsubduction porphyry Cu-Au and epithermal Au deposits: Products of remelting of subduction-modified lithosphere. Geology, 37: 247~250.

Rio-Salas R., Ochoa-Landin L, Valencia-Moreno M, Calmus T, Meza-Figueroa D, Salgado-Souto S, Kirk J, Ruiz J, Mendivil-Quijada H. 2017. New U-Pb and Re-Os geochronology of Laramide porphyry copper mineralization along the Cananea lineament, northeastern Sonora, Mexico: Contribution to the understanding of the Cananea copper district. Ore Geology Reviews, 81: 1125~1136.

Rioux M, Farmer G L, Bowring S A, Wooto, K M, Amato J M, Coleman D S, and Verplanck P. 2016, The link between volcanism and plutonism in epizonal magma systems: High precision U-Pb zircon geochronology from the Organ Mountains caldera and batholith, New Mexico. Contributions to Mineralogy and Petrology, 171: 1~22.

Saleeby J. 2003. Segmentation of the Laramide slabevidence from the southern Sierra Nevada region. Geological Society of America Bulletin, 115: 655~668.

Salvatierra-Domínguez E. 2000. Petrografía y geoquímica de los depósitos de tipo pórfido cuprífero de La Fortuna de Cobre y El Americano en el noroeste de México. Unpub. M. S. Thesis, Universidad de Sonora, 79.

Santillana-Villa C, Valencia-Moreno M, Rio-Salas R. 2021. Geochemical variations of precursor and ore-related intrusive rocks associated with porphyry copper deposits in Sonora, northwestern Mexico. Journal of South American Earth Sciences, 105: 1~22.

Singer D A, Berger V, Moring B C. 2008. Porphyry Copper Deposits of the World: Database and Grade and Tonnage Models. 2008. U. S. Geological Survey, Open-File. Report 2008~1155.

Talavera-Mendoza O, Ramírez-Espinoza J, Guerrero-Suástegui M. 1995. Petrology and geochemistry of the Teloloapan Subterrane: a lower Cretaceous evolved intra-oceanic island arc. Geofisica Internacional, 34: 3~22.

Talavera-Mendoza O, Guerrero-Suástegui M. 2000. Geochemistry and isotopic composition of the Guerrero Terrane (western Mexico): implication for the tectonomagmatic evolution of southwestern North America during the Late Mesozoic. Journal of South American Earth Sciences, 13: 297~324.

Tang Wei, Tang Zhengjiang, Cheng Zhimin, Gao Peng, Wang Qiuxuan. 2020&. Application of stream sediments geochemical survey in the Cu reconnaissance at the Tomatlan area, Mexico. East China Geology, 41(2): 159~165.

Titley S. 1995. Porphyry copper deposits of the American Cordillera. Arizona Geologocal Society Digest, 20: 6~20.

Tyler Resource Inc. 2008. Bahuérachi project preliminary economic assessment report, Chihuahua, Mexico. Technical Report, November 8, 138.

Wilkins J, Heidrick T L. 1995. Post Laramide extension and rotation in porphyry copper deposits, Southwestern United States. In: Bolm J G, ed. Porphyry copper deposits of the American Cordillera. Arizona Geological Society Digest 20, Tucson, 109~127.

Valencia-Moreno M, Iriondo A, Gonzalez-Leon C. 2006. Temporal constraints on the eastward migration of the Late Cretaceous-early Tertiary magmatic arc of NW Mexico based on new 40Ar/39Ar hornblende geochronology of granitic rocks. Journal of South American Earth Sciences, 22: 22~38.

Valencia V A, Eastoe C, Ruiz J, Ochoa Landín L, Gehrels G, Gonz'alez Le'on C, Arra F, Espinoza E. 2008. Hydrothermal evolution of the porphyry copper deposit at La Caridad, Sonora, Mexico, and the relationship with a neighboring high- sulfidation epithermal deposit. Economic Geology, 103 (3): 473~491.

Valencia-Moreno M, Ruiz J, Barton M D, Patchett P J, Zürcher L, Hodkinson D, Roldán-Quintana J. 2001. A chemical and isotopic study of the Laramide granitic belt of northwestern Mexico: identification of the southern edge of the North American Precambrian basement. Geological Society of America Bulletin, 113: 1409~1422.

Valencia-Moreno M, Ortega-Rivera A. 2011. Cretacico Tardio-Eoceno Medio en el noroeste de Mexico—evolucion del arco magmatico continental y su contexto geodinamico (orogenia Laramide). In: Calmus T, ed. Panorama de la geología de Sonora, Mexico, Universidad Nacional Autonoma de Mexico, Instituto de Geologia, Boletin, 118: 1~26.

Valencia V, Noguez-Alc'antara B, Barra F, Ruiz J, Gehrels G, Quintanar F, Valencia-Moreno M. 2005. U-Pb zircon and Re-Os molybdenite geochronology from La Caridad porphyry copper deposit: insights for the duration of magmatism and mineralization in the Nacozari District, Sonora, Mexico. Mineral Deposits, 40: 175~191.

Valencia V A, Noguez-Alcántara B, Barra F, Ruiz J, Gehrels G, Quintanar F, Valencia-Moreno M. 2006. Re-Os molybdenite and LA-ICPMS-MC U-Pb zircon geochronology for the Milpillas porphyry copper deposit: insights for the timing of mineralization in the Cananea District, Sonora, Mexico. Revista Mexicana de Ciencias Pecuarias, 23: 3~53.

Valencia-Moreno M, Ochoa-Landín L, Noguez-Alc'antara B, Ruiz J, P'erez-Segura E. 2007. Geological and metallogenetic characteristics of the porphyry copper deposits of Mexico and their situation in the world context. Geological Society of America, 422: 433~458.

Valencia-Moreno M, Lopez-Martinez M, Orozco-Esquivel T, Ferrari L, Calmus T, Noury M, Mendivil-Quijada H. 2021. The Cretaceous-Eocene Mexican Magmatic Arc: Conceptual framework from geochemical and geochronological data of plutonic rocks. Earth Science Reviews, 220: 1~18.

Yang Chao, Chen Xinghui, Zhao Xiaobo. 2020&. Exploration and prospecting potential of porphyry copper deposits in China. Geology of Shanxi, 38(2): 25~38.

Yang Zhiming, Hou Zengqian, Zhou Limin, Zhou Yiwei. 2020&. Critical elements in porphyry copper deposits of China. Science China Press, 65(33): 3653~3664.

Young J R, McMillan N J, Lawton T F, and Esser R P. 2000. Volcanology, geochemistry and structural geology of the Upper Cretaceous Hidalgo Formation, southwestern New Mexico. In: Lawton T F, McMillan N J, and McLemore VT, eds. Southwest Passage A trip through the Phanerozoic: New Mexico Geological Society Guidebook, 51: 149~156.

Zürcher L. 2002. Regional setting and magmatic evolution of Laramide porphyry copper systems in western Mexico. Unpub. Ph. D. Thesis, University of Arizona, 427.

Temporal and spatial distribution and typical deposit characteristics of Laramide porphyry copper deposits in Northern Mexico

YAO Chunyan[1), GUO Weimin[1), DING Haifen[2,3), LIU Jun'an[1), WANG Tiangang[1)

1) *Nanjing Center, China Geological Survey, Nanjing*, 210016;

2) *International Research Center of Big Data for Sustainable Development Goals, Beijing*, 100094;

3) *Key Laboratory of Digital Earth Science, Aerospace Information Research Institute, Chinese Academy of Sciences, Beijing*, 100094

Abstract: The porphyry copper belt in Sonora, northern Mexico, is an extension of the "large cluster" of North American porphyry copper ore concentration areas in Mexico, one of the world's important copper metallogenic provinces. Porphyry copper deposits are mainly distributed along the Laramide magmatic arc. During the Laramide (80~40 Ma) orogeny, due to the reduction of the subduction angle of the Farallon plate to the North American plate, the magmatic activity center gradually moved eastward, forming three magmatic activities of 76~70 Ma, 63~57 Ma and 46~40 Ma. During the peak period, the magma activity of 63~57 Ma was the largest. Through the comparative study on the metallogenic age of the existing deposits in the area, the time limit of magmatic activity and the distribution concentration of the deposits, it is found that the peak period of porphyry copper metallization is mainly concentrated in the period of 63~56 Ma. By combing the metallogenic characteristics of typical deposits and comprehensive analysis of regional magmatism, it is believed that the Laramide orogeny is the main geological process for the formation of huge copper and molybdenum enrichment in northern Mexico.

Keywords: Laramide orogeny; porphyry copper deposits; spatiotemporal distribution; northern Mexico

Acknowledgements: The writers sincerely thank to colleague Prof. YAO Zhongyou for his meaningful advices to this paper

First author: YAO Chunyan, born in 1980, Ph. D. on geochemistry at Nanjing University in 2010, a senior engineer of Nanjing Center, China Geological Survey, works on the geochemical survey and mineral geology; Email: ycyan@126. com

Corresponding author: WANG Tiangang, born in 1983, Ph. D. on mineral geology at Nanjing University in 2011, a senior engineer of Nanjing Center, China Geological Survey, works on the geochemical survey and mineral geology; Email: wangtg1897@163. com

Manuscript received on: 2022-07-01; Accepted on: 2022-08-11; Network published on: 2022-09-20

Doi: 10. 16509/j. georeview. 2022. 09. 061　　**Edited by**: LIU Zhiqiang